Calculation of thermodynamic properties of the Ni-Al alloys in normal conditions and under pressure

Calculation of thermodynamic properties of the Ni–Al alloys in normal conditions and under pressure

V Kuznetsov†, K Tsai‡ and T Turkebaev‡

† Institute of Strength Physics and Material Science, 634021 Tomsk, Russia
‡ Institute of Nuclear Physics NNC RK, 480082 Almaty, Kazakhstan

Abstract. We present an electron density model functional method (EDMF) based on the embedded atom theory and a pseudopotential approach to study thermodynamic properties and stability of binary metallic alloys. Test calculations of the pure Ni, Al and their alloys demonstrate the efficiency and accuracy of the method. The ground-state properties of ordered compounds and a disordered FCC phase in the Ni–Al system were obtained in normal conditions ($P = 0$) and under pressure. The results obtained at $P = 0$ are in quite good agreement with experimental data. Calculation under pressure predicts a change of compound stability with increasing pressure.

1. Introduction

Many problems in the theory of metallic systems require detailed understanding of the mechanisms of atomic bonds in metals and their alloys. Great progress in the theory of alloys has been made within the frameworks of the first-principle approaches, such as LMTO, ASW, KKR, LPPW etc. Interesting results for alloys with an ideal crystalline lattice and cubic symmetry of ordering were obtained. However, when considering the physical processes accompanied by distortions of the ideal structure the self-consistent models face insurmountable calculating difficulties. This caused the development of alternative theoretical approaches based on density functional ideas, such as the Finnis–Sinclair method and the embedded atom method (EAM). Semi-empirical embedded potentials of Finnis–Sinclair or EAM are widely used in calculations of crystalline defects, surface properties and processes related to the disruption of periodicity of a crystalline lattice. Despite their insufficient theoretical foundation these approaches take into account a many-body character of atomic interactions in solids and are very simple for calculation. The total energy is evaluated as a sum of pair and EAM-type potentials of atomic interactions. There is a certain freedom of choosing approximations for the energy terms and their quantitative contribution to the total energy. For properties of pure metals such ambiguity in the form of the total energy does not deteriorate the accuracy of calculations. However, for alloys it does not allow us often to obtain the exact results for energy of formation and other properties of experimentally observed phases, because the difference between the total energies of the competing phases is negligible. It is supposed that the main cause for the poor quantitative description of ideal alloys in EAM is due to the crude approximation of energy terms. Therefore, choice of a more correct expression for the total energy of alloys could yield a large dividend in accuracy of the results. An improved model has to give

not only good qualitative results for alloys, as in the EAM scheme [1], but also satisfactory quantitative data in comparison with the first-principle approaches. In this paper, we propose the electron density model functional method (EDMF) [2], based on the theses of the EAM and a pseudopotential approach. Our model uses inter-atomic potentials of EAM type. As the present work shows, the applied model yields quite accurate results for properties of the ground state of binary alloys with arbitrary structure in normal conditions ($P = 0$). Apart from this, it allows us to determine variations of the phase stability under pressure without any modification of the ordinary calculation scheme. This allows us to obtain new information about alloy structures under loading and can lead closely to understanding of the mechanisms of phase transformations.

The purpose of this work is to show the resources of the EDMF method, based on the EAM ideas, in qualitative and quantitative analyses for ideal binary alloys. Within the framework of this approach the complete calculation of the ordered phases and an FCC-disordered phase in the Ni–Al system were accomplished at $P = 0$ and with pressure increasing. The paper is organized as follows. In section 2, the basic theses of the EDMF method used in our calculations are presented. In section 3 we present the result obtained for the Ni–Al system in normal conditions. The results for thermodynamic stability of the Ni–Al alloys under pressure are presented in section 4.

2. Theory

In the EDMF method, the electron density of a crystal is represented as a sum of both $\rho_c(r)$, a core electron density, and $\rho_v(r)$, an almost free electron density. The core electrons are of internal filled shells and valence d electrons; the almost free (valence) electrons are of s, p shells. Taking into consideration such a density representation the total energy $E[\rho]$ can be expressed by

$$E = E_1[\rho_c] + E_2[\rho_v] + E_3[\rho_c, \rho_v] \tag{1}$$

where $E_1[\rho_c]$ is the energy of core electrons, consisting of Coulomb, kinetic and exchange terms; $E_2[\rho_v]$ is the energy of almost free electrons; $E_3[\rho_c, \rho_v]$ is the energy of interaction between the core and the almost free (valence) electron subsystems.

The energy of the core subsystem is taken, according to the Kim–Gordon approximation [3], as a sum of effective short-range potentials $V_{\alpha\beta}^C(R_{ij})$

$$E_1[\rho_c] = \frac{1}{2} \sum_{\alpha\beta} \sum_{i,j}^{N}{}' C_i^\alpha C_j^\beta V_{\alpha\beta}^C(R_{ij}) \tag{2}$$

where R_{ij} is a distance between the ith and jth atoms; N is the number of atoms in an alloy; C_i^α takes the value equal to 1 if the ith site is occupied by an atom of α type, and zero, otherwise. If core densities of neighbouring atoms do not overlap, the E_1 value is equal to zero. $E_2[\rho_v]$ in (1) is given in terms of the Thomas–Fermi approximation for almost free electron density

$$E_2[\rho_v] = E_q[\rho_v] + \int \mathcal{E}_{kxc}(\rho_v)\, dV + \int \mathcal{E}_k(\rho_v, \nabla\rho_v)\, dV \tag{3}$$

where the first term defines Coulomb energy, the second represents kinetic, exchange and correlation energies of the almost free electrons and the third term is a correction to the

kinetic energy caused by inhomogeneity of electron density. The Coulomb energy in the expression (3) for an alloy is determined as

$$E_q[\rho_\upsilon] = \sum_\alpha N_\alpha E_{qi}^\alpha + \frac{1}{2} \sum_{\alpha,\beta} \sum_{i,j}^N {}' C_i^\alpha C_j^\beta V_{\alpha\beta}^q (R_{ij})$$

where

$$E_{qi}^\alpha = \frac{1}{2} \iint_{VV'} \frac{\rho_\upsilon^\alpha(r)\rho_\upsilon^\alpha(r')}{|r - r'|} \, \mathrm{d}V \, \mathrm{d}V' - \int_V \frac{Z_i^{\alpha\upsilon}\rho_\upsilon^\alpha(r)}{r} \, \mathrm{d}V$$

$$V_q^{\alpha\beta}(R_{ij}) = \frac{Z_i^{\alpha\upsilon}Z_j^{\beta\upsilon}}{R_{ij}} + \frac{1}{2} \iint_{VV'} \frac{\rho_\upsilon^\alpha(|r - R_i|)\rho_\upsilon^\beta(|r - R_j|)}{|r - r'|} \, \mathrm{d}V \, \mathrm{d}V'$$

$$- \int_V \frac{Z_i^{\alpha\upsilon}\rho_\upsilon^\beta(|r - R_j|)}{|r - R_i|} \, \mathrm{d}V - \int_V \frac{Z_j^{\beta\upsilon}\rho_\upsilon^\alpha(|r - R_i|)}{|r - R_j|} \, \mathrm{d}V.$$

Here N_α is the number of α atoms in the alloy and $Z_i^{\alpha\upsilon}$ is the part of the charge of an α atom nucleus equal to the number of the almost free electrons.

By analogy with localized core electrons the density of almost free electrons can be written as

$$\rho_\upsilon(r) = \sum_\alpha \sum_j^N C_j^\alpha \rho_j^\alpha(|r - R_j|) \qquad \int \rho_\upsilon^\alpha(r) \, \mathrm{d}V = n_\upsilon^\alpha \tag{4}$$

where n_υ^α is the number of almost free electrons in atom α. The density $\rho_\upsilon^\alpha(r)$ can be written in terms of Slater's function superposition

$$\rho_\upsilon^\alpha(r) = \sum_{p=1}^{m=2} \frac{(\beta_p^\alpha)^{\nu_p^\alpha + 3}}{4\pi(\nu_p^\alpha + 2)!} N_p^\alpha r^{\nu_p^\alpha} \mathrm{e}^{-(\beta_p^\alpha r)}.$$

Here $\sum_{p=1}^m N_p^\alpha = n_\upsilon^\alpha$ and ν_p^α, β_p^α are parameters of Slater's functions. The effects of sd hybridization, as in the paper [4], were considered by means of fractional numbers n_υ^α obtained from the first-principle calculations. In this paper n_υ^α for Al was given equal to 3, and for Ni 1.4. Note that the electron density representation in terms of the Slater functions allows us to obtain the analytical expression for the Coulomb energy E_q in (3).

In terms of EAM potentials the total energy of a pure metal depends only on the volume V and the spaces $\{R_{ij}\}$ between atoms. To transform $E_2[\rho_\upsilon]$ to such form, let us write $\rho_\upsilon(r)$ as a sum of two terms

$$\rho_\upsilon(r) = \langle\rho_\upsilon\rangle + \Delta\rho_\upsilon(r)$$

where $\langle\rho_\upsilon\rangle$ is an averaged density of the almost free electrons in an alloy that depends on an atomic volume. Expanding $\mathcal{E}_{KXT}(\rho_\upsilon)$ by Taylor's theorem on $\Delta\rho_\upsilon(r)$ and truncating the series by the second term, we obtain

$$\int_V \mathcal{E}_{KXC}[\rho_\upsilon(r)] \, \mathrm{d}V = V \left\{ \mathcal{E}_{KXC}(\langle\rho_\upsilon\rangle) - \frac{1}{2}\langle\rho_\upsilon\rangle^2 \frac{\partial^2 \mathcal{E}_{KXC}}{\partial p^2} \bigg|_{\langle\rho_\upsilon\rangle} \right\}$$

$$+ \frac{1}{2} \frac{\partial^2 \mathcal{E}_{KXC}}{\partial\rho^2} \bigg|_{\langle\rho_\upsilon\rangle} \sum_\alpha N_\alpha \int_V [\rho_\upsilon^\alpha(r)]^2 \, \mathrm{d}V + \frac{1}{2} \sum_{\alpha,\beta} \sum_{ij}^N {}' C_i^\alpha C_j^\beta V_{\alpha\beta}^{KXC}(\langle\rho_\upsilon\rangle, R_{ij})$$

where

$$V_{\alpha\beta}^{KXC}(\langle\rho_\upsilon\rangle, R_{ij}) = \frac{\partial^2 \mathcal{E}_{KXC}}{\partial\rho^2} \bigg|_{\langle\rho_\upsilon\rangle} \int_V \rho_\upsilon^\alpha(|r - R_i|)\rho_\upsilon^\beta(|r - R_j|) \, \mathrm{d}V.$$

Making similar mathematical transformations for the last term of equation (3), one can show that

$$E_2[\rho_\upsilon(\boldsymbol{r})] = E_0(\langle\rho_\upsilon\rangle) + \frac{1}{2}\sum_{\alpha,\beta}\sum_{i,j}{}' C_i^\alpha C_j^\beta V_{\alpha\beta}^\upsilon(\langle\rho_\upsilon\rangle, R_{ij}) \tag{5}$$

where

$$V_{\alpha\beta}^\upsilon(\langle\rho_\upsilon\rangle, R_{ij}) = V_{\alpha\beta}^q(R_{ij}) + V_{\alpha\beta}^{KXC}(\langle\rho_\upsilon\rangle, R_{ij}) + V_{\alpha\beta}^g(\langle\rho_\upsilon\rangle, R_{ij}).$$

Here $E_0(\langle\rho_\upsilon\rangle)$ is a term depending only upon the volume and the averaged density $\langle\rho_\upsilon\rangle$; $V_{\alpha\beta}^\upsilon$ is an effective pair potential of almost free electron interaction.

The expression for $E_3[\rho_c, \rho_\upsilon]$ is searched as in a pseudopotential approach

$$E_3[\rho_c, \rho_\upsilon] = \sum_\alpha\sum_j^N C_j^\alpha \int_V W_{ps}^\alpha(\rho_\upsilon(\boldsymbol{r}), |\boldsymbol{r}-\boldsymbol{R}_j|)\rho_\upsilon(\boldsymbol{r})\,\mathrm{d}V. \tag{6}$$

Here W_{ps}^α is a norm-preserving pseudopotential of an α atom acting on a pseudodensity $\rho_\upsilon(r)$. Express the pseudodensity $\rho_\upsilon(r)$ at the jth atom in equation (6) as

$$\rho_\upsilon(\boldsymbol{r}) = \rho_\upsilon^\alpha(|\boldsymbol{r}-\boldsymbol{R}_j|) + \sum_{i\neq j}^N \rho_\upsilon^\alpha(|\boldsymbol{r}-\boldsymbol{R}_{ij}|). \tag{7}$$

According to the perturbation theory, expand equation (6) in terms of a small parameter, being the last term of equation (7). We obtain

$$E_3[\rho_c, \rho_\upsilon] = \sum_\alpha\sum_j^N C_j^\alpha \left\{ \int_V W_{ps}(|\boldsymbol{r}-\boldsymbol{R}_j|, \rho_\upsilon^\alpha(|\boldsymbol{r}-\boldsymbol{R}_j|))\rho_\upsilon^\alpha(|\boldsymbol{r}-\boldsymbol{R}_j|)\,\mathrm{d}V \right.$$
$$\left. + \sum_{k=0}^\infty \int_V f_k^\alpha(|\boldsymbol{r}-\boldsymbol{R}_j|)\left[\sum_\beta\sum_{i\neq j} C_i^\beta \rho_\upsilon^\beta(|\boldsymbol{r}-\boldsymbol{R}_{ij}|)\right]^{k+1}\mathrm{d}V \right\}$$

where $f_k^\alpha(r)$ are functions depending on the α-atom pseudopotential and its derivatives

$$f_k^\alpha(r) = \frac{1}{k!}\left\{\left.\frac{\partial^k W}{\partial\rho_\upsilon^k}\right|_{\rho_\upsilon^\alpha} + \frac{1}{k+1}\rho_\upsilon^\alpha(r)\left.\frac{\partial^{k+1}W}{\partial\rho_\upsilon^{k+1}}\right|_{\rho_\upsilon^\alpha}\right\}.$$

In the case of a pure metal E_3 can be written as

$$E_3[\rho_c, \rho_\upsilon] = \sum_j^N\left\{\int_V W_{ps}^\alpha(|\boldsymbol{r}-\boldsymbol{R}_j|, \rho_\upsilon^\alpha(|\boldsymbol{r}-\boldsymbol{R}_j|))\rho_\upsilon^\alpha(|\boldsymbol{r}-\boldsymbol{R}_j|)\,\mathrm{d}V + F_\alpha(\rho_\upsilon(R_j))\right\} \tag{8}$$

where the first term determines the core–valence interaction for isolated atom α. The electron density $\rho_\upsilon(R_j)$ at the jth atom's nucleus is a many-body function determined by the overall contribution of the electron 'tails' of neighbouring atoms. By analogy with EAM, the function $F_\alpha(\rho_\upsilon)$ can be considered as a local potential at the atom α, contributed by its interaction with all remaining atoms of the system. The potential $F_\alpha(\rho_\upsilon)$ for a metal of α type is obtained, as in EAM [5], through the equation of state, formulated for expanded or compressed metals [6]. Here the value of $F_\alpha(\rho_\upsilon)$ is the difference between the sublimation energy $E_{sub}^\alpha(\Omega)$, given by the equation of state, and the sum of the computed terms $E_1^\alpha[\rho_c^\alpha]$ and $E_\upsilon^\alpha[\rho_\upsilon^\alpha]$ for the pure component.

In order to obtain the expression for E_3 in case of a binary alloy, it is necessary to consider both the crystalline lattice of the alloy and the alloy's equilibrium volume per atom, Ω, instead of those in the case of the pure metal. Expanding the core–valence

interaction energy in equation (6) into a Taylor series in $\Delta\rho_\upsilon^\alpha(r)$ to the first order term one can obtain the following expression

$$\int_V W_{ps}^\alpha(r, \rho_\upsilon(r))\rho_\upsilon(r)\,\mathrm{d}V = \int_V W_{ps}^\alpha(r, \rho_\alpha^m(r))\rho_\alpha^m(r)\,\mathrm{d}V$$

$$+ \int_V \left\{ W_{ps}^\alpha(r, \rho_\alpha^m(r)) + \left.\frac{\partial W_{ps}^\alpha}{\partial \rho_\upsilon}\right|_{\rho_\alpha^m} \right\}\Delta\rho_\upsilon^\alpha(r)\,\mathrm{d}V$$

where $\Delta\rho_\upsilon^\alpha(r) = \sum_\beta \sum_j^N C_j^\beta \rho_\upsilon^\beta(|r - R_j|) - \sum_j^N \rho_\upsilon^\alpha(|r - R_j^\alpha|)$ is the difference between densities of the alloy and the pure metal. Here the first integrated expression is equivalent to the first term of equation (8) for pure metals being the alloy components. The second expression related to the alloy potential $F_\alpha(\rho_\upsilon)$ can be written as

$$F_\alpha(\rho_\upsilon(R_j)) = F_\alpha(\rho_\upsilon^m(R_j^\alpha)) + \Delta F_\alpha \tag{9}$$

where

$$\Delta F_\alpha = \gamma_\alpha \left.\frac{\partial F_\alpha}{\partial \rho_\upsilon}\right|_{\rho_\upsilon^m(R_j^\alpha)} (\bar\rho_\alpha(R_j) - \bar\rho_\alpha^m(R_j^\alpha)) \tag{10}$$

$$\bar\rho_\alpha(R_j) = \sum_{\beta=A,B}^N \sum_{i\neq j} C_j^\beta n_\upsilon^\beta \rho_\upsilon^\beta(R_{ij}) \qquad \bar\rho_\alpha^m(R_j^\alpha) = n_\upsilon^\alpha \sum_{i\neq j}^N \rho_\upsilon^\alpha(R_{ij}^\alpha). \tag{11}$$

The formulae (10) and (11) contain the so-called effective densities of almost free electrons given at atom's nucleus. Their designations are respectively $\bar\rho_\alpha(R_j)$ for an alloy, and $\bar\rho_\alpha^m(R_j^\alpha)$ for a pure metal. Here the contribution of the density from atom β is increased by the factor n_υ^β in comparison with the initial atomic density in (4).

The calculations show that computing the electron density at the atom α as

$$\rho_\upsilon^\alpha(R_j) = \sum_{\beta=A,B} \sum_{i\neq j}^N C_j^\beta \rho_\upsilon^\beta(R_{ij})$$

we obtain an incorrect result for the charge transfer between the components of an alloy in the Ni–Al system in the energy term of the core–valence interaction. For example, it is known that when forming NiAl alloy the electronic transfer goes from Al atoms to Ni atoms and is equal to 0.6 e (where e is the electron's charge) [7]. Let us compare the density values at the different atoms in the alloy NiAl (B2) (at the alloy's equilibrium volume) and in pure metals Ni and Al at their equilibrium volumes. For the case of the initial density $\rho_\upsilon^\alpha(R_j)$ we have a slight increasing of the electron density at the Ni atoms by the factor of 1.01, and a larger increasing, by the factor of 1.69, at the Al atoms. The main cause of this is the requirement that the electron density is calculated only at the point (atomic nucleus), not over the whole crystal. This, as well as in EAM, simplifies the calculation, but deteriorates the final results of the total energy computing. To obviate such a difficulty we introduced the effective densities giving more a correct pattern of redistribution of almost free electron charge between the different sorts of atom, when they have various n_υ. In this case $\bar\rho_{Ni}$ in the alloy NiAl (B2) increases by the factor of 1.96 in comparison with the pure metal and $\bar\rho_{Al}$ increases very slightly, by the factor of 1.01. This is in good qualitative agreement with the experimental result [7] and, further, leads to a more correct description of the Ni–Al phase diagram.

In our approach, the variation of the density when crystal structure changes from the lattice of a pure metal to an alloy is considered in term of the variation of the effective density $\Delta\bar\rho_\upsilon$. The values $\Delta\bar\rho_\upsilon$, $F_\alpha(\rho_\upsilon)$ and $(\partial F/\partial\rho)_{\rho_\upsilon^m}$ are defined for pure metals and only

Table 1. Equilibrium volumes Ω_0 and energies of formation ΔE for pure metals of various structures.

Structure	Al			Ni		
	Ω_0 (10^{-29}) $(m^3/atom)$	ΔE $(kJ\ mol^{-1})$	ΔE_γ $(kJ\ mol^{-1})$	Ω_0 (10^{-29}) $(m^3/atom)$	ΔE $(kJ\ mol^{-1})$	ΔE_γ $(kJ\ mol^{-1})$
A1	1.629	0.000	0.000	1.088	0.000	0.000
A2	1.636	1.441	1.063	1.094	3.909	0.008
A2[a]	1.603	5.225	—	1.035	3.046	—
D5$_{13}$	1.832	11.943	39.030	1.322	36.066	2.948
C16	1.757	11.395	23.803	1.232	32.900	3.263
C1	1.899	19.329	43.344	1.407	52.126	0.213
C15	1.712	7.989	16.225	1.177	23.572	2.796
D0$_{20}$	1.882	18.938	42.220	1.388	52.770	0.806

[a] Calculated volumes and energies from [9].

depend on the atomic arrangement $\{R_{ij}\}$ and volume Ω. Thus, the total energy of an alloy can be written as

$$E(\Omega) = E_0(\langle\rho_v\rangle) + \frac{1}{2}\sum_{\alpha\beta}\sum_{ij}^{N}{}' C_i^\alpha C_j^\beta V_{\alpha\beta}(\langle\rho_v\rangle, R_{ij})$$

$$+ \sum_{\alpha}\sum_{j}^{N} C_j^\alpha \{F_\alpha(\bar\rho_v) + \Delta F_\alpha(\bar\rho_v, \{R_{ij}\})\}. \tag{12}$$

Here the potential $F_\alpha(\Omega)$ corresponds to the variation of core–valence energy for pure metal α when its equilibrium volume Ω_α varies to be equal to the alloy one, Ω. The correction ΔF_α in (9) describes the variation of core–valence energy caused by both factors: redistribution of the density of almost free electrons at alloy formation and crystal structure transformation to the lattice of an alloy. The obtained expression (12) allows calculation of equilibrium volumes and energies for various crystal structures providing minimization of the total energy of an alloy on both the volume and lattice parameters. Unknown model parameters $\{\gamma_\alpha\}$ for any binary system can be obtained using the information on thermodynamic properties for a few phases in this system. $\{\gamma_\alpha\}$ are calculated to provide the theoretical results, being in good agreement with experimental data for formation energy ΔH and equilibrium volume Ω for any phase.

For accurate description of phase diagrams, it is necessary to ensure the energetic stability of the experimentally observed structures to be determined correctly over the whole range of composition. In particular, in the case of pure metals (Ni and Al), the theory must give the thermodynamic stability of FCC lattices. As shown, equation (12) gives the correct description for pure metals Al and Ni when passing from one crystalline structure to another. The results for formation energies ΔE of the pure metals in various structures are presented in table 1. The ground states of both Ni and Al are predicted to be FCC in comparison with the other calculated structures. The values ΔE are in reasonably good agreement with the results provided by LMTO [8] and the pseudo-potential approach [9] for a BCC structure. Here the values ΔE_γ, related to the core–valence contribution in ΔE, show that for Ni the stability of the FCC structure is caused by short-range repulsive interactions (2) between overlapping d-electron densities of neighbouring atoms. As follows from table 1, the contribution term ΔE_γ is very small for Ni, but for Al, where the core interactions are negligible, it is the main term determining the energy of a structure.

According to equation (12), the total energy of an alloy can be expressed as a functional of electron density distribution at different atoms and averaged atomic volume. At the same time, the electron density distribution is determined by the arrangement of atoms in the alloy, i.e. numbers of atoms of each kind on coordination spheres and atomic spaces $\{R_{ij}\}$. Thus, the total energy depends only on both the atomic volume and lattice parameters. Consequently, to determine the equilibrium structure characteristics for the ground state of an alloy it is necessary to minimize the total energy on the atomic volume and lattice parameters for all known structures. Such a procedure allows us not only to obtain the equilibrium parameters of the alloy, but also to investigate the phase stability at tetragonal and other distortions of the lattice.

3. Results for the Ni–Al system in normal conditions

The Ni–Al system in normal conditions ($P = 0$) [10], represented in figure 1, is characterized by a few solid phases: an FCC (A1) phase in both Al and Ni rich parts and ordered intermetallic compounds NiAl (B2), Ni_3Al (L1$_2$), $NiAl_3$(D0$_{20}$), Ni_2Al_3 (D5$_{13}$) and low-temperature Ni_5Al_3. Among the numerical attempts to describe these phases, the first-principle investigations [8, 11] allowed us to obtain the most accurate results. The list of the computed structures of alloys has included all the experimentally observed and also metastable ones. In [11] the energetic parameters for the possible structures, D0$_3$, D0$_{22}$, B32, D5, D7 and so on, were calculated. The formation energies and latter parameters for the complex phases D5$_{13}$, D0$_{20}$ firstly were described in the LMTO approach in [8]. In
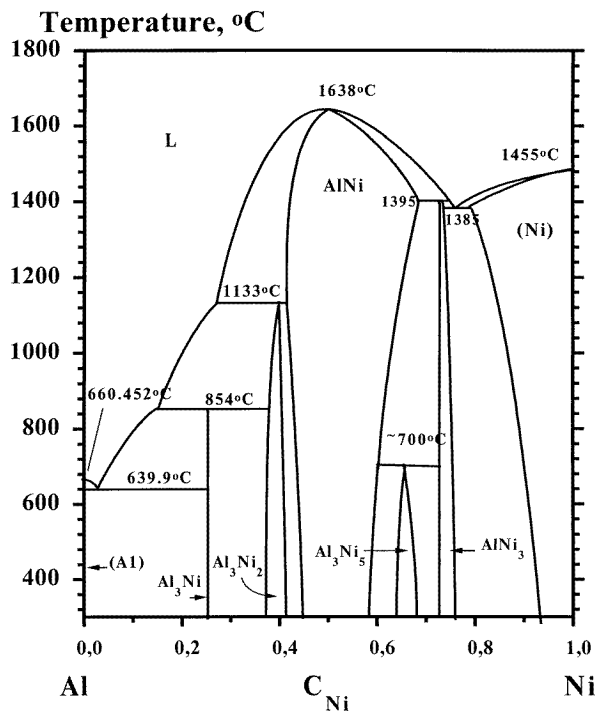

Figure 1. Experimental phase diagram of the Ni–Al system [10].

the present study, we also carry out the calculations for a wide list of competing structures for both phases, realized in the Ni–Al system and not realized. The coefficients $\{\gamma_\alpha\}$ in equation (12) for the Ni–Al alloys were obtained using a fit to the experimental quantities for both the formation energy $\Delta H = -59.073$ kJ mol^{-1} and the equilibrium volume $\Omega = 1.204 \times 10^{-29}$ m^3/atom for the NiAl (B2) alloy [12]. The computed parameters γ_α for Ni and Al are equal to 1.405 844 and 0.315 251, respectively.

The enthalpy of formation for a binary alloy is evaluated, as

$$\Delta H = E_{AB}(\Omega, \rho_A, \rho_B) + P\Omega - \sum_{\alpha=A,B} C_\alpha(E_\alpha(\Omega_\alpha) + P\Omega_\alpha) \qquad (13)$$

where E_{AB} is the total energy of an alloy; E_α is the energy of a pure metal in the experimentally observed structure; Ω_α, Ω are equilibrium volumes of a pure metal α and an alloy, respectively; C_α is a relative concentration of α-component in the alloy. Quantities $E_\alpha(\Omega_\alpha)$ and Ω_α are calculated for the pure metal α using the equation of state [6]. Pressure P and bulk modulus B for an alloy are calculated in terms of equation (13) and the formulae

$$P = -\partial E_{tot}/\partial \Omega \qquad B = \Omega\,\partial^2 E_{tot}/\partial \Omega^2.$$

Note, that in normal conditions, at $P = 0$, the equation (13) gives a value for the energy of formation of an alloy.

The results provided by the EDMF method for formation energies, equilibrium volumes and bulk moduli in the case of stable and metastable phases are presented in table 2. Note that for each structure, the total energy is obtained as a dependence on the atomic volume and its minimum determines values for both the equilibrium total energy and the equilibrium volume. As table 2 shows, all the results obtained are in good agreement with available experimental data [10, 12–14] for the ordered phases observed in the Ni–Al system. These are closely correlated with the theoretical results [11] for cubic structures and, in contrast to those, are more complete as extending to the complex structures, such as D0$_{20}$, D5$_{13}$ and others. At the same time the calculations [8] give the lowered values of ΔH for all the ordered phases (excepting D0$_{20}$) in comparison with experiment and our calculations.

The following intermediate ordered phases, such as B2 (NiAl), L1$_2$ (Ni$_3$Al), D0$_{20}$ (NiAl$_3$), D5$_{13}$ (Ni$_2$Al$_3$), are obtained to be stable. To describe the compound Ni$_5$Al$_3$ with narrow homogeneous region at low temperatures [10], we examined a BCC structure D5 isotypical with Ga$_3$Pt$_5$, as in [11]. However, the calculated ΔH(D5) is situated barely above the line connecting enthalpies of B2 and L1$_2$ (figure 2), so the D5 phase cannot be stable even at low temperatures. One can suppose that the real structure for the Ni$_5$Al$_3$ alloy differs from D5 and has an orthorhombic lattice, not a cubic one. In a similar way, our calculations do not confirm the stability of the Ni$_7$Al phase, denoted as D7 and isotypical with Ca$_7$Ge. The calculation [11], quite to the contrary, results in the energetic stability of undistorted structures D5 and D7. Additional EDMF calculations for alloys of the composition Ni$_2$Al and NiAl$_2$ with the structures C1, C15, C16, as one could expect, show their thermodynamic instability.

Apart from the listed intermetallic compounds, the Ni–Al system is characterized by the region of a disordered solid solution based on pure Ni. According to the calculations, this disordered phase is realized in the FCC lattice (A1) compared to the BCC one (A2). It is necessary to note that the calculation of the energy of disordered phases in terms of only the equation (12) is insufficient, because solid solutions are characterized by the effects of so-called static displacements of atoms leading to local distortions of lattice parameters and increasing the total energy. In order to view these effects and to calculate the energy of

Table 2. EDMF results for ΔH, B and Ω_0 of various structures in the Ni–Al system in comparison with LMTO results [8] and experimental data.

Composition	Structure	ΔH (kJ mol^{-1})	B (GPa)	c/a	Ω (10^{-29}) (m^3/atom)
Ni$_7$Al	D7	−18.237	185.38	1.00	1.111
Ni$_3$Al	L1$_2$	−37.292	182.32	1.00	1.133
	D0$_3$	−35.032	178.70	1.00	1.137
	D0$_{20}$	−24.811	153.72	0.77	1.219
	A2	−26.092	166.61	1.00	1.155
	A1	−27.048	170.67	1.00	1.149
	D0$_3$[a]	−46.732	—	1.00	1.084
	L1$_2$[a]	−48.360	—	1.00	1.102
	L1$_2$ (exp.)[b]	−38.332	174.7	1.00	1.128
Ni$_2$Al	C16	−33.386	153.69	1.06	1.251
	C15	−16.299	154.46	1.00	1.266
	C1	−32.724	152.34	1.00	1.353
Ni$_5$Al$_3$	D5	−46.657	169.84	1.00	1.170
	A1	−31.682	157.49	1.00	1.193
Ni$_3$Al$_2$	D5$_{13}$	−45.208	158.90	1.23	1.319
	A1	−31.960	154.81	1.00	1.204
NiAl	L1$_0$	−43.953	155.87	1.00	1.224
	B2	−59.073	164.02	1.00	1.204
	A2	−31.067	142.78	1.00	1.256
	A1	−31.143	144.57	1.00	1.250
	L1$_0$[a]	−56.185	—	1.00	1.179
	B2[a]	−75.599	—	1.00	1.175
	B2 (exp.)[b]	−59.073	165.9	1.00	1.204
Ni$_2$Al$_3$	D5$_{13}$	−57.099	153.60	1.24	1.409
	A1	−2.920	164.40	1.00	1.306
	D5$_{13}$[a]	−61.85	—	—	—
	D5$_{13}$ (exp.)[b]	−56.448	—	1.214	1.383
Ni$_3$Al$_5$	D3	−40.183	142.25	1.00	1.293
NiAl$_2$	C16	−49.937	145.98	0.91	1.379
	C15	−11.339	94.88	1.00	1.460
	C1	−47.757	137.33	1.00	1.477
NiAl$_3$	L1$_2$	−27.045	121.30	1.00	1.382
	D0$_3$	−25.801	120.30	1.00	1.386
	D0$_{20}$	−44.846	130.10	0.76	1.491
	A2	−18.058	111.44	1.00	1.411
	A1	−18.649	112.86	1.00	1.404
	L1$_2$[a]	−21.754	—	1.00	1.374
	D0$_3$[a]	−16.411	—	1.00	1.353
	D0$_{20}$[a]	−39.89	—	—	—
	D0$_{20}$ (exp.)[b]	−37.807	—	0.73	1.465
NiAl$_7$	D1	−10.911	96.85	1.00	1.497

[a] Calculated values in LMTO approach [8].
[b] Experimental values: energies of formation from [12]; bulk moduli from [13]; volumes from [14].

static lattice distortions the formula, resulting from [15, 16], was used in the present paper

$$\Delta H_r = -\frac{k_s}{16} B \frac{(\Omega_A - \Omega_B)^2}{\Omega} I_1 C_A C_B. \tag{14}$$
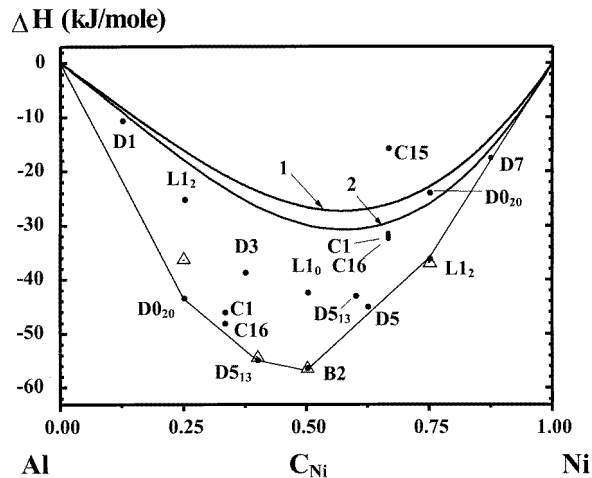
Figure 2. Enthalpy of formation as a function of composition for compounds and an FCC-disordered phase studied. Curves 1, 2—calculations without ΔH_r and with ΔH_r for the FCC solid solution. ●—EDMF-calculation for ordered phases, △—experiment [12].

Here $k_s = 4\sqrt{3}$ for BCC crystals and $k_s = 3\sqrt{2}$ for FCC crystals; B is a bulk modulus for an alloy, calculated in this work. The coefficient I_1, determined from the elastic moduli C_{11}, C_{12}, C_{44} for pure metals, is computed in the case of an alloy as the average by concentration of the values I_1^α for the alloy's components [15]. The quantities I_1^α for Ni and Al are equal to 0.243 and 0.262, correspondingly. The formation energy for the FCC solid solution is represented in figure 2 as a function of concentration. The minimum of this curve, in terms of the ΔH_r contribution, corresponds to $C_{Ni} = 0.58$.

4. Alloys of the Ni–Al system under pressure

As already mentioned, the calculated values of formation energy, equilibrium volume and bulk modulus of the Ni–Al alloys in normal conditions are in good agreement with the corresponding experimental data [10, 12–14]. Therefore, the results can be considered as factors speaking in favour of a reasonably satisfied physical correctness of all further calculations under pressure. As the calculation of ΔH values under pressure shows, the stability of any ordered phase in the Ni–Al system at $P = 0$ does not ensure this phase stability with outside pressure increasing (figure 3). The alloys referred to different parts of the phase diagram are predicted to have a dissimilar mechanism of stabilization directly associated with the quantitative composition of alloys. Based on the results obtained we can draw the following conclusions.

At the equiatomic composition the B2 ordered phase (NiAl) is thermodynamically favoured at the overall interval of outside pressure (0–50 GPa). In addition this structure is stable with respect to the tetragonal distortion in the [001] crystal direction. For Ni-rich alloys the increasing of outside pressure also is not followed by any phase equilibria changes. Among all the possible intermetallic compounds, the only Ni₃Al phase with the $L1_2$ structure is predicted to be stable at various pressures. Such phases as D5 (Ni₅Al₃) and D7 (Ni₇Al) are unstable both in normal conditions and under pressure, though their formation enthalpies are located very close to the connodes, connecting ΔH of the thermodynamically stable phases.
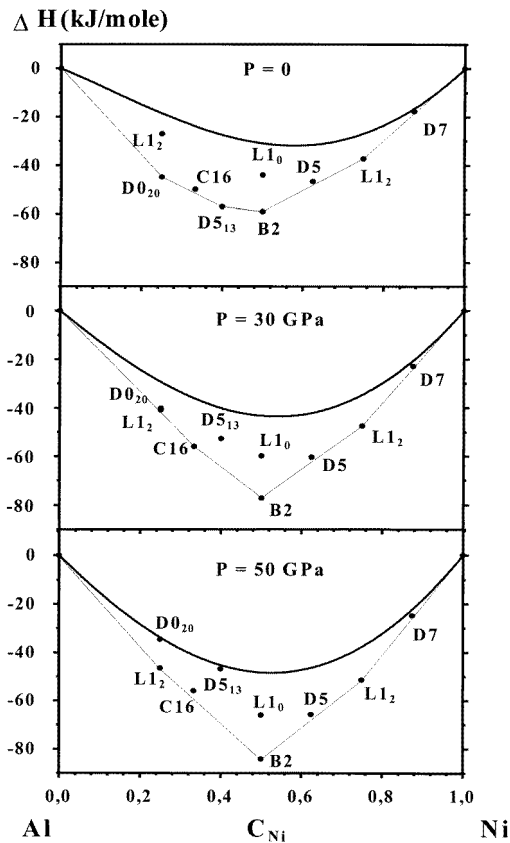
Figure 3. Concentration-dependent enthalpy of formation of the Ni–Al alloys at $P = 0$, 30 and 50 GPa. The curves correspond to the case of a disordered FCC phase (A1) with regard to static lattice distortions.

For Al-rich alloys the analysis predicts their more complex behaviour with pressure. It is caused by both the great variety of structural modifications of the competing phases for this part of the phase diagram and the fact that the requirement of close packing is not fulfilled for their structures. The calculations indicate that at zero temperature and for pressure increasing the Al-rich alloys have a possible change in the composition of phase equilibria and appearance of new stable ordered phases, not observed at normal pressure (figure 4). According to the calculations, the alloy at $C_{Ni} = 0.33$ at $P = 0$ is a heterogeneous mixture of both DO_{20} and $D5_{13}$. Conditions for a Laves phase C16 (NiAl$_2$) stabilization appear with increasing pressure. The pressure value required for the stability of C16 varies between 4 and 40 GPa. The structure ratio c/a obtained for this structure is equal to 0.91, not varying with increasing pressure. The ordered hexagonal phase $D5_{13}$ is predicted to become thermodynamically unstable even at small pressures. Its enthalpy of formation is decreasing in absolute value with rising pressure. When P is greater than 6.3 GPa, $D5_{13}$ is less stable with regard to a mixture of NiAl$_2$ (C16) and NiAl (B2). Consequently, in the Ni$_2$Al$_3$ alloy under pressure the lamination of the $D5_{13}$ phase is possible followed by the precipitation of both the ordered compound NiAl$_2$ (C16) and NiAl (B2): $D5_{13}$ (Ni$_2$Al$_3$) $\rightarrow$ C16 (NiAl$_2$)+B2 (NiAl). The variations of lattice parameters a and
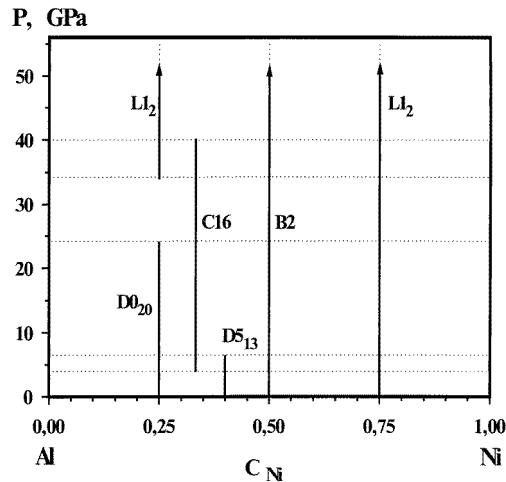
Figure 4. The phase diagram (pressure–composition) for the Ni–Al system at $T = 0$ K.
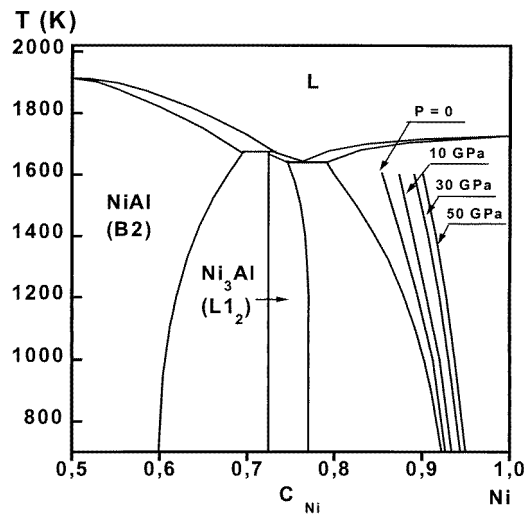

Figure 5. The evolution of the boundary of the homogeneity region for the Ni-based solid solution under pressure.

c for the D5$_{13}$ structure are negligibly small under pressure. The calculation also predicts a limited stability for the D0$_{20}$ (NiAl$_3$) orthorhombic phase. This phase is calculated to be stable at pressure varying up to 24 GPa. At 24 GPa there is a point of equilibrium of three phases: pure Al (A1), D0$_{20}$ (NiAl$_3$) and C16 (NiAl$_2$). With further pressure increasing the disappearance of the orthorhombic structure D0$_{20}$ is favoured resulting in the formation of the mixture from two phases: NiAl$_2$ (C16) and pure Al. At pressure of 34 GPa the possible structural transition of the NiAl$_3$ alloy to the close-packed FCC-structure L1$_2$ was obtained. A new phase L1$_2$ kept stable when pressure was increased up to 50 GPa. Therefore for the alloy at $C_{Ni} = 0.25$ our calculation provides the following consequence of phase-structural transitions under pressure: D0$_{20}$ (NiAl$_3$) $\rightarrow$ A1 (Al) + C16 (NiAl$_2$) $\rightarrow$ L1$_2$ (NiAl$_3$).

The calculation of the formation enthalpy for a disordered phase in the Ni–Al system shows the FCC solid solution (A1) to be more favoured in comparison with the BCC one (A2) at an arbitrary alloy's composition and pressure value. To estimate the boundary of the homogeneity region for the Ni-based disordered phase its Gibbs energy was calculated in term of the model of regular solid solutions

$$G = \Delta H + kT[C_A \ln C_A + (1 - C_A) \ln(1 - C_A)].$$

Here ΔH obtained at $T = 0$ K were used for the alloys $Ni_{1-x}Al_x$ and Ni_3Al; the energy contribution from the heat lattice oscillations to ΔH is not taken into consideration. Considering that the Gibbs energy of the Ni_3Al is equal to ΔH of the compound Ni_3Al ($L1_2$), the tangent lines are drawn from the point with coordinates $\Delta H(L1_2)$, $C_{Ni} = 0.75$ to the curves of the disordered phase at the temperature interval from zero to 1600 K. The coordinates of the points of tangency determine the boundary of the homogeneity region at various temperatures (figure 5). The resulting curve at $P = 0$ is in agreement with the one on the experimental phase diagram. All computations under pressure were carried out keeping the value of the coefficient I_1 in (14) as constant and equal to one at normal pressure. As figure 5 shows, the increasing of the outside pressure results in a little decreasing of ΔH_r values. At $P = 0$ the minimum of the curve of ΔH (with ΔH_r) takes place at $C_{Ni} = 0.58$. At higher pressures the location of the curve minimum is displaced to the middle of the concentration interval. For instance, at $P = 30$ GPa the formation enthalpy for the disordered solid solution has a minimum at $C_{Ni} = 0.54$, and at 50 GPa it has one at $C_{Ni} = 0.52$. The theoretical estimation of the solubility boundary under pressure gives some displacement to pure nickel. The greater is the value of outside pressure the stronger is this displacement and the narrower is the region of homogeneity of the FCC solid solution.

Table 3. The values $\Delta\Omega$ obtained for the ordered phases under pressure. $\Delta\Omega = \Omega - \Omega_V$ (10^{29}) (m^3/atom).

	$P = 0$ GPa	$P = 10$ GPa	$P = 30$ GPa	$P = 50$ GPa
NiAl B2	−0.154	−0.115	−0.075	−0.054
Ni$_3$Al L1$_2$	−0.090	−0.066	−0.042	−0.030
NiAl$_2$ C16	−0.069	−0.036	−0.013	0.001
Ni$_2$Al$_3$ D5$_{13}$	−0.004	0.026	0.040	0.047
NiAl$_3$ D0$_{20}$	−0.002	0.031	0.042	0.046
NiAl$_3$ L1$_2$	−0.112	−0.081	−0.057	−0.042

Table 4. The results obtained in normal conditions for energies and pressures of the predicted phase transitions.

Phase transition state 1 → state 2	$E_1 - E_2$ (kJ mol^{-1})	$\Delta\Omega_1$	$\Delta\Omega_2$	$\Delta\Omega_1 - \Delta\Omega_2$ ($\times 10^{-29}$) (m^3/atom)	P_{teor} (GPa)	P^* (GPa)
D0$_{20}$ → Al + C16	−7.112	−0.002	−0.052	0.050	24.0	21.5
Al + C16 → L1$_2$	10.017	−0.052	−0.112	0.060	34.0	39.6
D0$_{20}$ + D5$_{13}$ → C16	−1.650	−0.003	−0.069	0.066	4.4	4.0
C16 → L1$_2$ + B2	−11.758	−0.069	−0.126	0.056	40.0	31.1
D5$_{13}$ → C16 + B2	−3.375	−0.004	−0.103	0.100	6.3	6.0
D0$_{20}$ → L1$_2$	−17.132	−0.002	−0.112	0.110	28.0	27.3

Analysis of the results obtained for the Ni–Al binary system has indicated that the energy of formation, $\Delta E(P)$, for all viewed ordered phases increased in absolute value with pressure rising, but the difference between ΔE values for the competing phases changed slightly. Therefore the main factor in equation (13) responsible for changes of phase stability under pressure is

$$P\left(\Omega - \sum_{\alpha=A,B} C_\alpha \Omega_\alpha\right).$$

Here the parenthetical term determines a deviation of the alloy's equilibrium volume from Vegard's volume Ω_V calculated at the same pressure P. The greater is the negative deviation $\Delta\Omega$ of alloy equilibrium volume from Vegard's rule, the greater is the increase of the formation enthalpy in the negative range of values. This results in increasing of the probability of phase stability with pressure rise. The calculated values of $\Delta\Omega$ at various pressures for the considered ordered phases are represented in table 3. The table shows that the stable intermetallides NiAl (B2), Ni_3Al ($L1_2$) have high negative variation $\Delta\Omega$ at all pressures, whereas for the phases $D0_{20}$, $D5_{13}$, $\Delta\Omega$ is small and changes its sign with pressure rise. Our calculation for the $NiAl_3$ alloy gives the greater negative variation $\Delta\Omega$ for the $L1_2$ structure, than for $D0_{20}$. The first-principles calculations [8] at $P = 0$ for the $NiAl_3$ alloy gave similar results: $\Delta\Omega(L1_2) = -0.119 \times 10^{-29}$ m^3/atom and $\Delta\Omega(D0_{20}) = -0.079 \times 10^{-29}$ m^3/atom. Formation energy values ΔE for the phases $D0_{20}$ and $L1_2$ change with pressure very slightly. For instance, at pressure rising up to 50 GPa $\Delta E(D0_{20})$ increased by the factor 1.08 in magnitude, and $\Delta E(L1_2)$ by 1.25. The latter is not enough to stabilize the close-packed $L1_2$ structure at $P < 50$ GPa. Therefore, the stability under pressure of the $L1_2$ ($NiAl_3$) phase is also caused by greater negative variation of its equilibrium volume from Vegard's rule. Our calculation predicts the phase transition $D0_{20} \to L1_2$ at 28 GPa.

The enthalpy of alloy formation can be approximated as

$$\Delta H(P) = \Delta E(0) + P\Delta\Omega(0) - \frac{1}{2}P^2\left(\frac{\Omega_0}{B_0} - \sum_{\alpha=A,B} \frac{\Omega_0^\alpha}{B_0^\alpha}\right) \qquad (15)$$

where Ω_0, B_0, $\Delta E(0)$ are an equilibrium volume, a bulk modulus and a formation energy of an alloy, correspondingly, at $P = 0$; Ω_0^α, B_0^α are a volume and a bulk modulus for a pure metal of α type when there is no pressure. The equation (15) includes the values of thermodynamic properties of alloys evaluated merely in normal conditions. Hence, this fact can be easily used to estimate approximately the critical pressure values for stable and metastable phase transitions. The accuracy of determination of phase transition pressure depends on the accuracy of the results (ΔH, Ω, B) obtained in normal conditions. Table 4 introduces the calculated energy differences for both start and final phase states of alloys, the volume variation from Vegard's rule for these phases in normal conditions and critical pressures of phase transitions estimated due to equation (15), P^*, in comparison with the detailed results P_{teor}. For two-phase alloys the concentration-mean values of formation energies and volume variations are presented. As table 4 shows, the obtained results for pressures of phase transitions due to equation (15) differ by 5–10% from the accurate calculation under pressure. It follows that to predict possible phase transitions and critical pressure values it is sufficient to make the accurate computation of formation enthalpies, equilibrium volumes and bulk moduli of the competing phases in normal conditions. This allows us to simplify the needed calculations and is valid for the phase transitions not caused by electronic transformations. It is necessary to note that the basic conclusions of the present

analysis for features of the alloys in the Ni–Al system, obtained in normal conditions, are legitimate at P not equal to zero.

5. Conclusion

It should be mentioned that the EDMF approach proposed in this paper resembles closely the embedded atom method [5]. In the EDMF expression for core–valence interactions, consisting of the terms F_α and ΔF_α, the idea of EAM, to calculate the embedded potential as a function of $\rho_v(0)$ in terms of the state equation, was used. In this connection, the terms of the core–valence energy in the present work are denoted by the F_α symbol, as an embedded function in EAM. It has been shown with the example of the Ni–Al system that the EDMF method allows evaluation of thermodynamic properties and stability of alloys with various structures including complex ones not only in normal conditions, but also under pressure. Nevertheless, this approach is not self-consistent; the correctness of the obtained results is compared with that of the known first-principle calculations. The results are in very good agreement with appropriate experimental data. On the other hand, the EDMF method is similar to the EAM semi-empirical approach. This demonstrates the possibility in principle to improve the calculation scheme of the semi-empirical potentials. This will give a possibility to fulfil more correct calculations in the case of many-component metallic systems and to obtain a more detailed pattern of phase transformations under pressure.

References

[1] Johnson R A 1990 *Phys. Rev.* B **41** 9717
[2] Tsai K V, Kuznetsov V M, Kaminskii P P, Turkebaev T E and Zambarny S A 1996 *Izv. Vyzov Fiz.* **4** 91
[3] Gordon R G and Kim Y S 1972 *J. Chem. Phys.* **56** 3122
[4] Hausleitner Ch and Hafner J 1990 *J. Phys.: Condens. Matter* **2** 6651
[5] Foiles S, Baskes M and Daw M 1986 *Phys. Rev.* B **33** 7983
[6] Rose J, Smith J R, Guinea F and Ferrante J 1984 *Phys. Rev.* B **29** 2963
[7] Muller Ch, Wonn H, Blau W, Ziesche P and Krivitski V 1979 *Phys. Status Solidi* b **95** 215
[8] Pasturel A, Colinet C, Paxton A T and Schilfgaarde M 1992 *J. Phys.: Condens. Matter* **4** 945
[9] Dagens L 1977 *Phys. Status Solidi* b **84** 311
[10] Desai P D 1987 *J. Phys. Chem. Ref. Data* **16** 116
[11] Lu Z W, Wei S-H and Zunger A 1991 *Phys. Rev.* B **44** 512
[12] Haltgren R, Desai D D and Hawkins D T 1973 *Selected Values of Thermodynamic Properties of Binary Alloys* (Metal Park, OH: ASM) p 1435
[13] Rubini S and Ballone P 1993 *Phys. Rev.* B **48** 99
[14] Barabash O and Koval Yu 1986 *Structura i Svoistva Metallov i Splavov* (Kiev: Naukova Dumka)
[15] Froyen J and Herring C 1972 *Phil. Mag.* **26** 7165
[16] Hafner J and Panz G 1983 *J. Phys. F: Met. Phys.* **13** 1393